

# TIME-RESOLVED RESONANCE RAMAN CHARACTERIZATION OF THE $bL_{550}$ INTERMEDIATE AND THE TWO DARK-ADAPTED $bR_{560}^{DA}$ FORMS OF BACTERIORHODOPSIN

JAMES TERNER, CHUNG-LU HSIEH, AND M. A. EL-SAYED, *Department of  
Chemistry, University of California, Los Angeles, Los Angeles, California  
90024 U.S.A.*

**ABSTRACT** The resonance Raman spectrum of the second intermediate in the bacteriorhodopsin cycle,  $bL_{550}$ , is obtained by a simple flow technique. The Schiff base linkage in this intermediate appears to be protonated, contrary to previous suggestion. The fingerprint region of the spectrum of  $bL_{550}$  does not closely match those of any presently available model Schiff bases of retinal isomers, though some comparisons can be made. The resonance Raman spectrum of dark-adapted bacteriorhodopsin is obtained and decomposed by computer subtraction of the spectrum of  $bR_{570}$ . The remaining spectrum does not match the spectra of any model compounds presently in the literature. The spectra of  $bL_{550}$  and dark-adapted  $bR_{560}^{DA}$  from purple membrane in  $H_2O$  are compared to those in  $D_2O$ . It is found that changes in the spectrum occur in the  $1,600\text{--}1,650\text{ cm}^{-1}$  region as well as in the  $800\text{--}1,000\text{ cm}^{-1}$  region, but apparently not in the fingerprint region ( $1,100\text{--}1,400\text{ cm}^{-1}$ ). The possibilities of conformational changes of the retinal chromophore in the light adaptation process as well as the photosynthetic cycle are discussed.

## INTRODUCTION

Bacteriorhodopsin is a retinal protein complex similar in structure to the visual pigments. Besides the chlorophylls, it is the only biological system known to be able to convert solar energy to chemical energy (1). While under illumination, bacteriorhodopsin cycles through several intermediates (Fig. 1), pumping protons from inside of the cell membrane to the outside. The resultant electrochemical gradient is thought to drive the phosphorylation of ADP. In addition to the light-adapted cycle there is a reversible conversion to a dark-adapted state ( $bR_{560}^{DA}$  in Fig. 1). This mechanism is thought to be the one by which the bacteria are able to locate regions of illumination and to avoid regions of intense or ultraviolet light (2).

The kinetics of the photochemical cycle of bacteriorhodopsin (Fig. 1) have been extensively characterized by flash photolytic techniques. A recent review is given by Stoeckenius et al. (3). Because the transient absorptions are broad and structureless, resonance Raman spectroscopy is presently being used to obtain more detailed information about the intermediates in the cycle. The beginning resonance Raman work on bacteriorhodopsin studied the two intermediates,  $bR_{570}$  and  $bM_{412}$ , which had the largest steady-state concentrations while under laser illumination (4–7). Some of the more recent resonance Raman work on bacteriorhodopsin has been what is called time-resolved or kinetic resonance Raman spectroscopy (8–11). These methods are designed to obtain resonance Raman spectra of transient

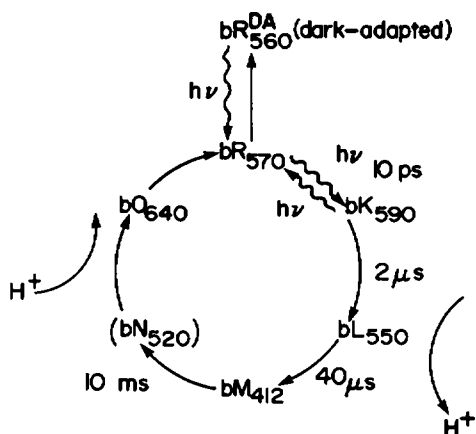


FIGURE 1 Photochemical cycle of bacteriorhodopsin as suggested by the work described in reference 3. Half times are given for room temperature. Subscripts are absorption maxima in nanometers.

intermediates as they occur during the functioning cycle as opposed to trapping a species by chemical means or at low temperatures, and may be more representative of actual physiological conditions. Also recently, the molecular flow technique has been used to obtain resonance Raman spectra of unphotolyzed  $bR_{570}$ , and  $bM_{412}$  stabilized at high pH (11). The molecular flow technique was previously used to obtain the spectra of unphotolyzed rhodopsin and retinal isomers (12–14). At present, essentially complete spectra of  $bR_{570}$ ,  $bM_{412}$  and the dark-adapted  $bR_{560}^{DA}$  form have been published (8, 11, 15), and features of  $bK_{590}$  and  $bL_{550}$  (7, 10, 15) as well as  $bM_{412}$  and  $bR_{570}$  (4–6) have been reported and discussed.

In this report we present the complete spectrum of the  $bL_{550}$  intermediate, and resolve the  $bR_{560}^{DA}$  spectrum by computer subtraction, to derive the spectra of its component retinal isomers. We also discuss the effect of suspension of the purple membrane in  $D_2O$  on the spectra of various bacteriorhodopsin forms. Aside from previously discussed shifts of  $C=N$  stretching frequencies (6), additional bands appear in the  $800\text{--}1,000\text{ cm}^{-1}$  region in protonated intermediates. Besides confirming the existence of a photolabile proton on the chromophore, these bands are unique to each species providing a “deuteration fingerprint” that can be used for identification of particular intermediates in future studies. This is especially useful inasmuch as ethylenic stretching frequencies most frequently used for identifying particular intermediates, as well as the  $1,150$  to  $1,400\text{ cm}^{-1}$  fingerprint regions, are sometimes very similar, making differentiation difficult.

## EXPERIMENT

### Samples

*Halobacterium halobium* S-9, a mutant strain believed to contain little carotenoid, was the gift of Dr. Janos Lanyi of National Aeronautics and Space Administration/Ames Research Center, Moffett Field, California. The purple membrane was grown and isolated by the methods of Becher and Cassium (16) and suspended at  $\approx 50\text{ }\mu\text{M}$  in deionized water. Additional samples of purple membrane were generously donated by Professor Walther Stoeckenius of the University of California, San Francisco.

Preparations were assayed for carotenoid content by resonance Raman spectroscopy. 100 mW of 5,145 Å excitation will reveal shoulders at 1,515 and 1,155  $\text{cm}^{-1}$  if a sufficient amount of carotenoid is present. The scan is done quickly since prolonged laser irradiation will cause the carotenoid to decompose. Resonance Raman spectroscopy is a more sensitive detector for carotenoid than optical absorption. Samples that appear carotenoid free by absorption may show clear carotenoid bands in the resonance Raman spectra. Only those preparations that had insufficient carotenoid to show up by our assay were used for these studies.

### *Apparatus*

The resonance Raman spectrometer used is a modified version of that described previously (8, 9). Laser light from a Spectra Physics model 165 argon ion laser or a model 375 dye laser (Spectra-Physics Inc., Laser Products Div., Mountain View, Calif.) was focused vertically across the sample. Scattered light was collected and focused onto the slit of a Spex 1870 0.5-M spectrograph (Spex Industries, Inc., Metuchen, N.J.) fitted with a 1,200 groove/mm ruled grating. A glass cutoff filter (Corning Glass Works, Science Products Div., Corning, N.Y.) was used to minimize Rayleigh scattered radiation. A 100- $\mu\text{m}$  slit width resulted in 5  $\text{cm}^{-1}$  resolution.

Our detection system, an Optical Multichannel Analyzer (OMA; Princeton Applied Research Corp., Princeton, N.J. 1205A) with a silicon intensified vidicon (Princeton Applied Research Corp., 1205D), has been improved by the addition of a dry ice-cooled housing (Princeton Applied Research Corp., 1212) and an extended delay accessory (Princeton Applied Research Corp., 1207). Cooling the vidicon decreases the preamplifier dark noise significantly, resulting in the ability to scan for several hours without saturating the memory. Statistical noise in the data is thus reduced by eliminating the need to subtract large amounts of dark current. The extended delay accessory allows us to reduce the number of counts that originate from the vidicon scanning filament, another source of statistical noise. With these accessories we are able to obtain spectra with excellent signal: noise ratios with count rates of 0.1 count/s in 1 or 2 h. The extended delay accessory reduces, but does not eliminate, the considerable lag between accumulation of data on the vidicon target and the readout into memory; this lag causes a serious distortion of the spectrum. Because of this, we discard the first one-third (or more if necessary) of our data to let the target equilibrate with the signal before actual data is accumulated, thus avoiding distortion of the spectra, which would invariably result in inaccurate computer subtractions.

The use of the OMA requires displaying our spectra in segments. Additionally, with our present apparatus we cannot observe bands below  $\approx 800 \text{ cm}^{-1}$  due to the limitations imposed by using a cutoff filter with a single spectrograph as opposed to the double monochromators normally used for Raman spectroscopy. Digital data from the OMA is transferred to a PDP 11/45 computer (Digital Equipment Corp., Marlboro, Mass.) for analysis and display purposes. We have not smoothed any spectra shown in this paper. Absolute vibrational energies are accurate to  $\pm 5 \text{ cm}^{-1}$ .

### *bL<sub>550</sub>*

To identify the resonance Raman spectrum of bL<sub>550</sub> we have used two methods. The first is the laser pulse time-resolved method described previously by this laboratory (8, 9). It uses a rotating chopper to obtain pulses from a continuous wave (cw) laser; the pulses impinge on a stationary sample in a melting point capillary. This method has enabled us to follow the kinetic behavior of various bands and correlate them with the kinetics of the known intermediates that have been characterized by flash photolysis (3). The second method, a variant of methods used by others (10–13), makes use of a cw laser beam impinging on a jet stream of bacteriorhodopsin. Instead of varying the flow rate (10), we keep the flow rate constant but vary the incident laser power.

All spectra of bL<sub>550</sub> shown in this paper have been obtained by the power-dependent flow method. We have found it a more effective way of observing the weak bands than the pulsed laser method. For these experiments, 3 ml of bacteriorhodopsin at 50  $\mu\text{M}$  in deionized water were recirculated by means of a peristaltic pump (Cole-Parmer Masterflex, Cole-Palmer Instrument Co., Chicago, Ill.). The sample was forced through a 25-gauge syringe needle that had an internal diameter of 0.25 mm. At the bulk flow

rate of 0.5 ml/s we estimate the jet velocity to be 10 m/s. With a 100- $\mu\text{m}$  beam waist, the time a molecule spends in the beam is 10  $\mu\text{s}$ . The sample reservoir was continuously illuminated by a flashlight to insure that we were monitoring the light-adapted cycle.

Obtaining the resonance Raman spectrum of  $\text{bL}_{550}$  is difficult because it is always superimposed on  $\text{bR}_{570}$ , and very weak. Care must be taken not to mistake weak contributions from  $\text{bM}_{412}$  and  $\text{bO}_{640}$ , which can be as strong as the  $\text{bL}_{550}$  bands. Identification of the presence of these intermediates is made by observing a band at  $1,567\text{ cm}^{-1}$  for  $\text{bM}_{412}$  (5–11) and broadening of the  $1,530\text{ cm}^{-1}$  band of  $\text{bR}_{570}$  at  $1,520\text{ cm}^{-1}$  for  $\text{bO}_{640}$ <sup>1</sup> and  $\text{bK}_{590}$  (7).<sup>2</sup> To obtain the  $\text{bL}_{550}$  bands we first obtained a spectrum where the bands of  $\text{bL}_{550}$  were maximized in relation to the bands of  $\text{bR}_{570}$  while avoiding contributions from other intermediates. The 10  $\mu\text{s}$  laser interaction time was effective for avoiding contributions from  $\text{bM}_{412}$  and  $\text{bO}_{640}$ . An additional spectrum of  $\text{bR}_{570}$  with as little as possible of  $\text{bL}_{550}$  was then obtained and computer-subtracted from the first spectrum.

There is a contribution to our spectra from the intermediate  $\text{bK}_{590}$  ( $t_{1/2} = 2\text{ }\mu\text{s}$ ) since the laser interaction time is 10  $\mu\text{s}$ . Though we have not been able to totally avoid the  $\text{bK}_{590}$  peaks, they have been characterized by this laboratory<sup>2</sup> and are noted as such in this paper (see Results and Discussion). We performed our experiments at 4,765, 4,880, 4,965, 5,145, 5,287, and 5,530 Å. The chosen excitation frequency for Figs. 2–6 was 5,145 Å to minimize the resonance enhancements of  $\text{bK}_{590}$  and  $\text{bO}_{640}$  while still being able to take advantage of the resonance enhancement of  $\text{bL}_{550}$ . Contributions from  $\text{bM}_{412}$  appeared when 4,765 Å was used.

We have found that the Raman peak of water at  $1,640\text{ cm}^{-1}$ , though weak and broad, appears clearly in our spectra as a shoulder at  $1,620\text{ cm}^{-1}$ , especially at high power (see Results and Discussion). We have subtracted the water peak from the spectra of Fig. 5, but not from Fig. 2.

It has been shown by Hurley et al. (17) that  $\text{bL}_{550}$  is photosensitive. Photoproducts of  $\text{bL}_{550}$  might be produced at our power densities, but if they occur would probably not be able to reach significant concentration since the irradiated sample has been completely removed from the detection area in 10  $\mu\text{s}$ . The photoproducts seen by Hurley et al. (17) were allowed to accumulate in a stationary sample at 77°K.

### $\text{bR}_{560}^{\text{DA}}$

The experimental arrangement for the dark-adapted experiments was identical to that used to obtain  $\text{bL}_{550}$ , minus illumination of the reservoir. Typically 3 ml of sample was used and laser power levels were 1 mW. A complete scan was taken in 20 min, after 12 h of dark adaptation. Some light adaptation was noticeable but unavoidable because of the small amounts of bacteriorhodopsin available. Light adaptation was evidenced by decreases in the intensity of the 1,183 and  $1,536\text{ cm}^{-1}$  dark-adapted bands. 5,145 Å excitation (15) gave results identical to those obtained at 5,287 Å.

### Computer Subtraction

The interpretation of computer-subtracted spectra must be made with caution. When spectra are subtracted, the noise from both of the original spectra is added (18). Subtracting two spectra with excellent signal:noise ratios may result in a difference spectrum of marginal quality. If the differences are small, the noise level may become larger than features of interest. We have tried to obtain original spectra with the largest possible signal:noise ratio and with differences maximized. We also have been careful to subtract only spectra taken under conditions as identical as possible. Subtracting a flow spectrum from a stationary sample spectrum may show differences that are due to polarized scattering from different average orientations of the molecules.

Normalization of the subtraction is not a cut-and-dry procedure. Certain bands peculiar to a certain species can be monitored. When these peaks disappear the subtraction can be said to have been

<sup>1</sup>Terner, J., C. L. Hsieh, A. R. Burns, and M. A. El-Sayed. 1979. Time-resolved resonance Raman characterization of the  $\text{bO}_{640}$  intermediate; reprotonation of the Schiff base. Submitted for publication.

<sup>2</sup>Terner, J., C. L. Hsieh, A. R. Burns, and M. A. El-Sayed. 1979. Time-resolved resonance Raman characterization of the intermediates of bacteriorhodopsin: the  $\text{bK}_{590}$  intermediate. Submitted for publication. (see Table I)

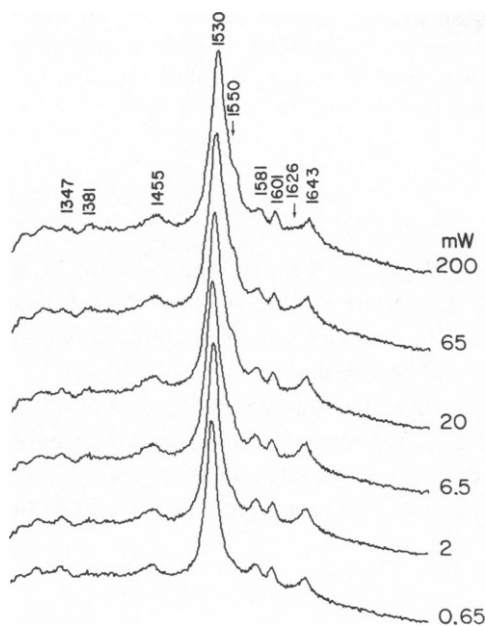


FIGURE 2

FIGURE 2 Power-dependent resonance Raman flow spectra in the range 1,300–1,700  $\text{cm}^{-1}$ , using 5,145 Å excitation, showing the accumulation of  $\text{bL}_{530}$  bands. 1,626  $\text{cm}^{-1}$  feature is a shoulder of the 1,640  $\text{cm}^{-1}$  Raman water band.

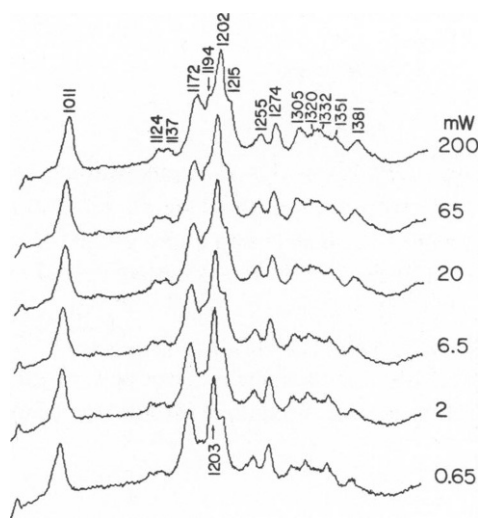


FIGURE 3

FIGURE 3 Power-dependent resonance Raman flow spectra in the range 1,000–1,400  $\text{cm}^{-1}$ , using 5,145 Å excitation, showing the accumulation of  $\text{bL}_{530}$  bands.

normalized. Details of this procedure are described in Results. For the purposes of clarity and to avoid inaccurate normalization due to our personal bias, we have shown a series of subtractions by a series of arbitrarily unnormalized weighting factors. It should be noted that the weighting factors depend only upon the length of time used to accumulate a spectrum and contain no quantitative information. Subtracted spectra where oversubtraction has caused negative peaks have been eliminated. For the computer-subtracted spectra in this paper it is our opinion that a subtraction has been completed just before peaks go negative.

We feel that our computer-subtracted spectra should be regarded as aids that help identify features in real data, rather than as actual data. However, we feel that the reliability of the computer-generated peaks described in this paper is quite good. If the lag problem of the OMA is not taken into account, large peaks will appear to be too tall, and small features will appear too weak. We have not smoothed any difference spectra so that all features may be judged in relation to the noise level, but it should be noted that features that remain after subtracting very large peaks (i.e., the 1,547  $\text{cm}^{-1}$  band in Fig. 5 b) have a much greater noise level than the base-line noise level, because the statistical fluctuations of the large signals have been added to the small remainder. In general, the computer-derived peaks of  $\text{bR}_{560}^{\text{DA3}}$  have a higher reliability level than the  $\text{bL}_{530}$  peaks, because the  $\text{bR}_{560}^{\text{DA}}$  features are much stronger in the original spectra than the  $\text{bL}_{530}$  peaks. Peaks that are not superimposed on  $\text{bR}_{570}$  peaks, such as the 967 and 986  $\text{cm}^{-1}$  peaks of Fig. 6 b, even though they are weak, are very reliable. Peaks that are superimposed on  $\text{bR}_{570}$  peaks, such as the 1,522 and 1,647  $\text{cm}^{-1}$  peaks of Fig. 5 b, are not as reliable and

<sup>3</sup>In this paper we call  $\text{bR}_{530}^{\text{DA}}$  one of the two forms present in  $\text{bR}_{560}^{\text{DA}}$ , assuming the other form to contain the same isomer as in  $\text{bR}_{570}$ .

must be checked carefully (we feel though that these features are quite real because we have reproduced them reliably in many experiments). The 1,122 and 1,135  $\text{cm}^{-1}$  peaks of Fig. 6 *b* and 1,382 and 1,602  $\text{cm}^{-1}$  peaks of Fig. 8 *b* are least reliable because they are the difference of very small peaks in the original spectra. These features may be real, but they could be artifacts of the lag of the OMA.

## RESULTS

### A. $bL_{550}$

Some features of the resonance Raman spectrum of  $bL_{550}$  have already been identified: the C=C stretch as a shoulder at 1,555  $\text{cm}^{-1}$  (8, 10), a band at 1,620  $\text{cm}^{-1}$  (9) that was previously assigned as an unprotonated C=N stretch (6), and a band in the fingerprint region at 1,190  $\text{cm}^{-1}$  (15). The complete spectrum of  $bL_{550}$  will now be described.

Figs. 2–4 show the results of flow experiments where the interaction time of flowing bacteriorhodopsin with the laser beam is 10  $\mu\text{s}$ . The 0.65-mW spectra contain essentially pure  $bR_{570}$  because the incident laser power is too low to cause a significant amount of photolysis on a 10- $\mu\text{s}$  pass of the sample through the beam. As incident laser power is increased from 0.65 to

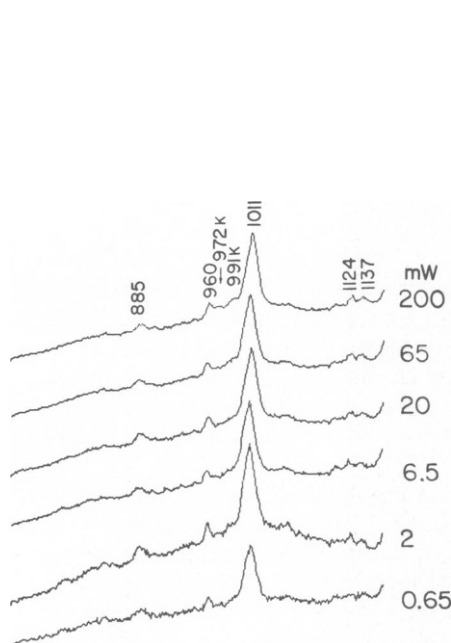


FIGURE 4

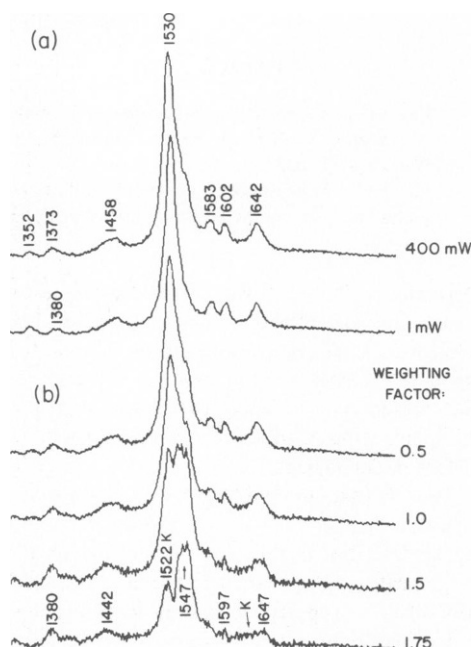


FIGURE 5

FIGURE 4 Power-dependent resonance Raman flow spectra in the range 750–1,150  $\text{cm}^{-1}$ , using 5,145 Å excitation; bands of  $bK_{590}$  are denoted by K.

FIGURE 5 Computer subtraction to obtain the resonance Raman spectrum of  $bL_{550}$  in the range 1,300–1,700  $\text{cm}^{-1}$ . (a) High and low power flow spectra using 5,145 Å excitation. The high power spectrum contains  $bL_{550}$  superimposed on  $bR_{570}$ . The low power spectrum contains pure  $bR_{570}$ . The Raman spectrum of water has been subtracted from these two spectra. (b) Computer subtraction of spectra in *a* by arbitrary weighting factors leaving the resonance Raman spectrum of  $bL_{550}$ .  $bK_{590}$  bands are denoted by K.

200 mW, the amount of photolysis is increased and  $bL_{550}$  grows into the spectrum superimposed on the  $bR_{570}$  bands. The bacteriorhodopsin ( $t_{1/2} = 10$  ms) is allowed to relax for several seconds before each pass through the laser beam so that there is no steady-state accumulation of intermediates.

Computer subtractions used to visualize  $bL_{550}$  are shown in Figs. 5, 6, and 7. Spectra obtained using low-incident laser power that contain essentially pure  $bR_{570}$  are subtracted from high-power spectra that contain  $bL_{550}$  superimposed on  $bR_{570}$ . We have chosen the  $1,352\text{ cm}^{-1}$  band to assist in normalization of the subtractions. As can be seen in Fig. 3, the  $1,352\text{ cm}^{-1}$  band does not grow as power is increased and, when it is totally subtracted, no negative bands appear (Figs. 5 and 6). It thus appears to be due to  $bR_{570}$  alone and not  $bL_{550}$ . When the  $1,352\text{ cm}^{-1}$  band is subtracted, we have assumed that we have subtracted the spectrum of  $bR_{570}$ .

### The $1,400\text{--}1,700\text{-cm}^{-1}$ Region

The growth of the  $1,550\text{ cm}^{-1}$  C=C stretch (8) and a band at  $1,626\text{ cm}^{-1}$  previously assigned to  $bL_{550}$  (9) can be seen in the power-dependent flow spectra of Fig. 2. We have determined

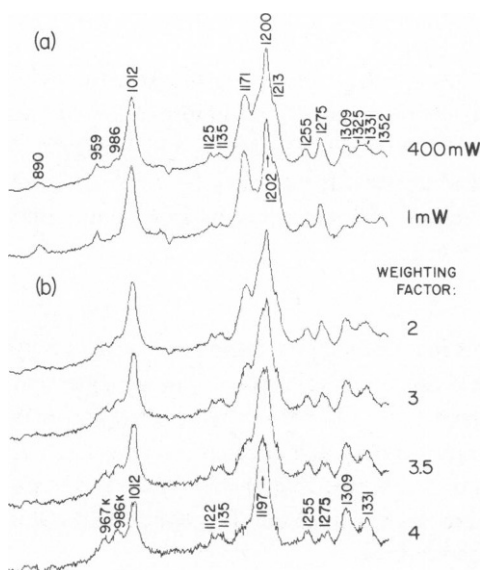


FIGURE 6

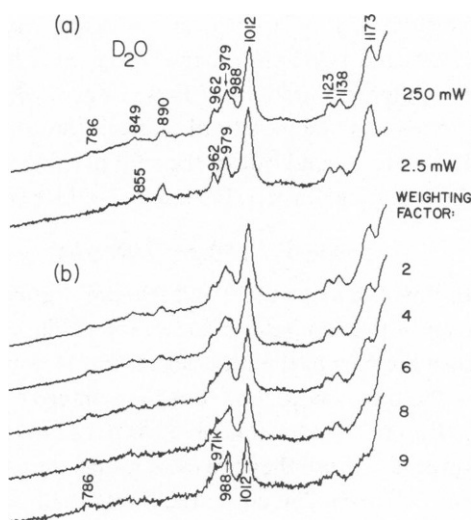


FIGURE 7

FIGURE 6 Computer subtraction to obtain the resonance Raman spectrum of  $bL_{550}$  in the range  $800\text{--}1,350\text{ cm}^{-1}$ . (a) High and low power resonance Raman flow spectra using  $5,145\text{ Å}$  excitation. The high power spectrum contains  $bL_{550}$  superimposed on  $bR_{570}$ . The low power spectrum contains pure  $bR_{570}$ . (b) Computer subtraction of spectra in a by arbitrary weighting factors leaving the resonance Raman spectrum of  $bL_{550}$ . The inverted peak between  $1,012$  and  $1,122\text{ cm}^{-1}$  is an artifact.  $bK_{590}$  bands are denoted by K.

FIGURE 7 Computer subtraction to obtain the resonance Raman spectrum of  $bL_{550}$  in the range  $750\text{--}1,180\text{ cm}^{-1}$  for  $D_2O$  suspension. (a) High and low power spectra using  $5,145\text{ Å}$  excitation. The high power spectrum contains  $bL_{550}$  superimposed on  $bR_{570}$ . The low power spectrum contains pure  $bR_{570}$ . (b) Computer subtraction of spectra in a by arbitrary weighting factors leaving  $bL_{550}$  resonance Raman bands.

that the  $1,626\text{ cm}^{-1}$  band has a large contribution from a broad water band centered at  $1,640\text{ cm}^{-1}$ . A  $\text{bK}_{590}$  band<sup>2</sup> is also present in this region. We have removed the water band from Fig. 5 by subtracting water spectra from the two spectra shown in Fig. 5a; it is not subtracted from Fig. 2. Computer subtractions in Fig. 5b show that a band at  $1,647\text{ cm}^{-1}$  is due to  $\text{bL}_{550}$  and most probably is a protonated Schiff base vibration as confirmed by deuteration studies (see heading labeled Deuteration Studies of  $\text{bL}_{550}$  in Results). A residual  $1,442\text{ cm}^{-1}$  band can also be assigned to  $\text{bL}_{550}$ .

A band at  $1,522\text{ cm}^{-1}$  is the C=C stretch of  $\text{bK}_{590}$  (7),<sup>2</sup> though it should be mentioned that it may possibly be due to difficulties caused by subtraction of large numbers (the  $1,530\text{-cm}^{-1}$  bands). We have estimated that  $\text{bK}_{590}$  should be expected to be present in significant concentration during a  $10\text{-}\mu\text{s}$  laser interaction time. The weakness of the  $1,522\text{-cm}^{-1}$  band is due to excitation frequency considerably removed from the absorption maximum.

The  $1,547\text{-cm}^{-1}$  ethylenic stretch of  $\text{bL}_{550}$  does not have the clean peaked shape of the ethylenic stretches characteristic of retinals and rhodopsins (4–15). It is possible that this band may be a superposition of multiple bands (19).<sup>4</sup> The  $1,581\text{-cm}^{-1}$  band may be due to  $\text{bR}_{570}$  alone. A band at  $1,597\text{ cm}^{-1}$  appears in repeated experiments that may be due to  $\text{bL}_{550}$ ; however, it is very close to the noise level.

#### *The 1,000–1,400- $\text{cm}^{-1}$ Region*

Most readily apparent from the power-dependent flow spectra of Fig. 3 is the growth of the  $1,194\text{-}$  and  $1,332\text{-cm}^{-1}$  bands assigned to  $\text{bL}_{550}$ . These features can be seen more clearly in the computer subtractions of Figs. 5 and 6. Bands at  $1,255$ ,  $1,275$ ,  $1,309$ ,  $1,331$ , and  $1,380\text{ cm}^{-1}$  can also be assigned to  $\text{bL}_{550}$  from the computer subtractions. It may also be noted that the  $1,197\text{-cm}^{-1}$  band causes the shift of the  $1,202\text{-cm}^{-1}$  band to lower energy by 1 or  $2\text{ cm}^{-1}$ , and the rounding of the  $1,215\text{ cm}^{-1}$  shoulder (Figs. 3 and 6a).

#### *The 800–1,150- $\text{cm}^{-1}$ Region*

In Fig. 4, bands at  $972$  and  $991\text{ cm}^{-1}$  grow as power increases. These bands are more clearly seen in the computer subtraction of Fig. 6. The behavior of these bands might indicate that they are part of the  $\text{bL}_{550}$  spectrum. However, we have determined that they are strong peaks in the  $\text{bK}_{590}$  spectrum.<sup>2</sup> The  $\text{bL}_{550}$  intermediate appears to possess a carbon-methyl stretch at  $1,012\text{ cm}^{-1}$  and weak bands at  $1,122$  and  $1,135\text{ cm}^{-1}$  (Fig. 6), though the weak bands are suspect because they are close to the noise level. There appear to be no  $\text{bL}_{550}$  bands below  $960\text{ cm}^{-1}$  down to  $750\text{ cm}^{-1}$ , the limit of our detection capabilities.

#### *Deuteration Studies of $\text{bL}_{550}$*

Deuteration effects on the resonance Raman spectrum of bacteriorhodopsin have been previously reported (4–6, 8). Suspension of purple membrane in  $\text{D}_2\text{O}$  has some interesting

<sup>4</sup>Marcus and Lewis (19) suggest that what we have (8, 9) identified as the  $\text{bL}_{550}$  intermediate is actually a new intermediate that they have called  $X$  ( $\lambda_{\text{max}}$  between  $460$  and  $485\text{ nm}$ ), which appears before the  $\text{bM}_{412}$  intermediate; and have resolved a C=C stretch of  $\text{bL}_{550}$  at  $1,537\text{ cm}^{-1}$ . It is difficult, at this time, to assign these bands conclusively to the corresponding intermediates. It is conceivable that one of these bands could be due to the  $\text{bN}_{520}$  intermediate, and the possibility of the presence of  $\text{bL}_{550}$  photoproducts cannot be eliminated. We would like to point out, however, that other bands assigned to  $X$  or  $\text{bL}_{550}$  by Marcus and Lewis at  $973$ ,  $1,165$ ,  $1,225$ , and  $1,237\text{ cm}^{-1}$  do not appear in our spectra of  $\text{bL}_{550}$ .



effects on the spectrum of  $\text{bL}_{550}$ . No apparent effect is seen in the fingerprint region (20). In the 1,600- to 1,650- $\text{cm}^{-1}$  region a repetition of the experiment of Fig. 5 shows shifts that are characteristic of protonated Schiff bases. A high-power flow spectrum (containing  $\text{bL}_{550}$  superimposed on  $\text{bR}_{570}$ ) shows a shift from 1,642- to 1,622- $\text{cm}^{-1}$ . The low-power flow spectrum ( $\text{bR}_{570}$  only) shows a deuteration shift from 1,642- to 1,625- $\text{cm}^{-1}$ . The resultant difference spectrum reveals a band at 1,619  $\text{cm}^{-1}$  belonging to  $\text{bL}_{550}$  (these spectra are shown in reference 20). The  $\text{bL}_{550}$  intermediate displays a deuteration band at 988  $\text{cm}^{-1}$  (Fig. 7). We have found that protonated forms of bacteriorhodopsin show deuteration effects between 950 and 1,000  $\text{cm}^{-1}$ . Along with reduction in the intensities of the 1,012  $\text{cm}^{-1}$  bands,  $\text{bR}_{570}$  shows a new band at 979  $\text{cm}^{-1}$  (8), and  $\text{bR}_{560}^{\text{DA}}$  at 991  $\text{cm}^{-1}$  (Fig. 11). The  $\text{bO}_{640}^1$  and  $\text{bK}_{590}^2$  intermediates which we have found to possess protonated Schiff bases also show deuteration effects in this region. The unprotonated intermediate,  $\text{bM}_{412}$  (8,20), shows no such effect that we have been able to detect. These additional deuteration effects confirm the existence of an exchangeable proton coupled to the chromophore and is evident in the spectrum of  $\text{bL}_{550}$  (Fig. 7) at 988  $\text{cm}^{-1}$ . It is also suggested that the extra bands in this region, which appear upon deuteration, be used as fingerprints to identify protonated retinal intermediates.

### B. $\text{bR}_{560}^{\text{DA}}$

It has been suggested that the dark-adapted form  $\text{bR}_{560}^{\text{DA}}$  is an equilibrium mixture of two isomers, 13-*cis* and all-*trans* retinal. It has been shown (21, 22) that reconstitution of 13-*cis* retinal into bacterio-opsin results in an absorption maximum at 550 nm and that all-*trans* retinal reconstituted into bacterio-opsin gives an absorption maximum of 570 nm and is identical to  $\text{bR}_{570}$ . The resonance Raman spectrum of  $\text{bR}_{560}^{\text{DA}}$  supports the proposal of two isomers in equilibrium, though the identity of the two isomers within the protein matrix is not yet clear.

Assuming that one of the isomers of  $\text{bR}_{560}^{\text{DA}}$  is in fact that of  $\text{bR}_{570}$ , we have subtracted the spectrum of  $\text{bR}_{570}$  from  $\text{bR}_{560}^{\text{DA}}$ . For the purposes of our discussion we call the remainder  $\text{bR}_{550}^{\text{DA}}$  (as opposed to  $\text{bR}_{560}^{\text{DA}}$ ).

#### *The 1,400–1,700- $\text{cm}^{-1}$ Region*

The most evident change in this region of the spectrum upon dark adaptation is the broadening of the C=C stretch at 1,530  $\text{cm}^{-1}$  from 16 to 26  $\text{cm}^{-1}$  (Fig. 8 *a*), which is indicative of two species. Computer subtraction shown in Fig. 8 *b* shows a C=C stretch at 1,536  $\text{cm}^{-1}$  that correlates well with a 550-nm absorption maximum by the inverse linear correlation of  $\nu_{\text{C}=\text{C}}$  with  $\lambda_{\text{max}}$  of Heyde et al. (23) and could correspond to the reconstituted 13-*cis* retinal absorption at 550 nm (21, 22). Also from the computer subtraction (Fig. 8 *b*) the 1,453 and 1,644  $\text{cm}^{-1}$  bands appear to be part of the spectrum of the  $\text{bR}_{550}^{\text{DA}}$  but not the band at 1,582. The shift of the 1,644  $\text{cm}^{-1}$  band to 1,622  $\text{cm}^{-1}$  upon suspension of the purple membrane in  $\text{D}_2\text{O}$  (20) suggests that the Schiff base is protonated in both isomers of  $\text{bR}_{560}^{\text{DA}}$ .

#### *The 1,000–1,400- $\text{cm}^{-1}$ Region*

The region from 1,000 to 1,400  $\text{cm}^{-1}$  of the dark-adapted form  $\text{bR}_{560}^{\text{DA}}$  in comparison with the same region of  $\text{bR}_{570}$  is shown in Fig. 9 *a*. Several changes are apparent on dark adaptation. A new band appears at 1,183  $\text{cm}^{-1}$ , and there is an apparent increase in intensity of the 1,202  $\text{cm}^{-1}$  band causing a rounding out of the shoulder at 1,213  $\text{cm}^{-1}$ . Bands in the region from

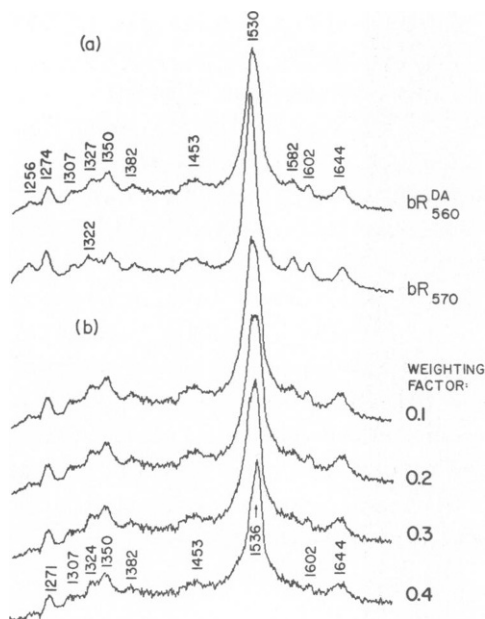


FIGURE 8

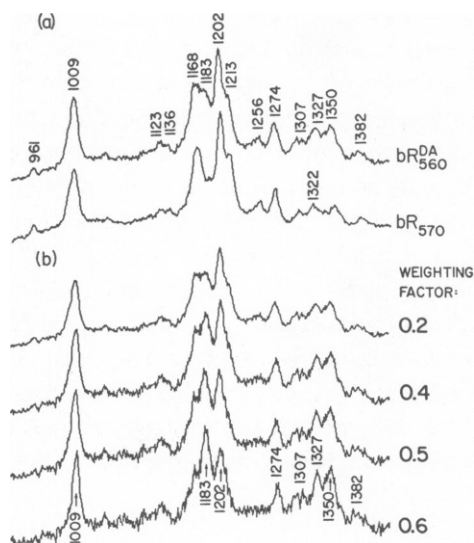


FIGURE 9

FIGURE 8 (a) Comparison of the resonance Raman spectra of dark-adapted  $bR_{560}^{DA}$  and light-adapted  $bR_{570}$  obtained with a recirculating flow sample and 1 mW of 5,287 Å excitation in the range 1,200–1,700  $\text{cm}^{-1}$ . (b) Computer subtraction of the spectra in a by arbitrary weighting factors leaving the resonance Raman spectrum of  $bR_{560}^{DA}$ .

FIGURE 9 (a) Comparison of the resonance Raman spectra of dark-adapted  $bR_{560}^{DA}$  and light-adapted  $bR_{570}$  using 1 mW of 5,287 Å excitation and a recirculating flow sample, for the range 950–1,400  $\text{cm}^{-1}$ . (b) Computer subtraction of the spectra in a by arbitrary weighting factors leaving the resonance Raman spectrum of  $bR_{560}^{DA}$ .

1,250 to 1,380  $\text{cm}^{-1}$  change in intensity. The band at 1,256  $\text{cm}^{-1}$  loses approximately half of its intensity in relation to the other bands as compared to the spectrum of  $bR_{570}$ . This band appears to be due to  $bR_{570}$  alone and is used as an internal standard for normalization purposes. Finally a band at 1,322  $\text{cm}^{-1}$  in the  $bR_{570}$  spectrum shifts to 1,327  $\text{cm}^{-1}$  upon dark adaptation. These features, though subtle, are reproducible in repetitive experiments.

Computer subtraction of the two spectra of Fig. 9 a are shown in Fig. 9 b. (Though the weighting factors in Figs. 8 b, 9 b, 10 b, and 11 b are arbitrary and unnormalized, the actual normalized weighting factors are, in fact, approximately one half, in agreement with the results of Dencher et al. [21] and Sperling et al. [22].)

### The 800–1,000- $\text{cm}^{-1}$ Region

As shown in Fig. 10 a, dark-adapted bacteriorhodopsin exhibits a weak band at 806  $\text{cm}^{-1}$  which is not seen in  $bR_{570}$ . This could be an out-of-plane bending mode or torsional vibration of a *cis*-retinal as predicted by Warshel and Karplus (24); however, this vibration exhibits a shift in frequency to 815  $\text{cm}^{-1}$  upon suspension of the purple membrane in  $D_2O$ . The shift

TABLE I  
COMPARISON OF THE VIBRATIONAL ENERGIES OF  $bR_{570}$ ,  $bL_{550}$ ,  $bR_{560}^{DA}$ , AND  $bR_{550}^{DA}$

$bR_{570}$	$bL_{550}$	$bR_{560}^{DA}$	$bR_{550}^{DA}$
$cm^{-1}$			
885(vw)		806(m) [815(m)]	806(m) [815(m)]
959(w)		888(vw)	
	967(w) K[971(m)] K	961(w)	
[979(m)]		[979(m)]	
	986(w) K		
	[988(m)]		
		[991(m)]	[991(s)]
1,012(s)	1,012(s)	1,009(s)	1,009(s)
1,125(w)	1,122(w)?	1,123(w)	?
1,135(w)	1,135(w)?	1,136(w)	?
1,171(s)		1,168(s)	
		1,183(s)	1,183(s)
	1,197(s)		
1,202(s)		1,202(s)	1,202(s)
1,213(m)		1,213(m)	
1,255(w)	1,255(w)	1,256(vw)	
1,275(m)	1,275(w)	1,274(m)	1,274(m)
1,309(w)	1,309(w)	1,307(w)	1,307(m)
1,325(m)			
	1,331(m)		
		1,327(m)	1,327(m)
1,352(m)		1,350(m)	1,350(m)
1,377(m)	1,380(m)	1,382(m)	1,382(w)
1,456(m)	1,442(m)	1,453(m)	1,453(m)
1,530(vs)	1,522(s) K	1,530(vs)	
			1,536(vs)
	1,547(s)		
1,581(m)		1,582(m)	
	1,597(w)		
1,600(m)		1,602(m)	1,602(w)?
1,642(m) [1,625]	1,647(m) [1,619(m)]	1,644(m) [1,622(m)]	1,644(m) [1,622(m)]

Letters in parentheses denote intensity: vw, very weak; w, weak; m, medium; s, strong; vs, very strong. Energies in  $D_2O$  suspensions are noted in brackets.  $bK_{590}$  bands determined from footnote 2 are labeled K. Absolute energies are accurate to  $\pm 5\text{ cm}^{-1}$ .

might indicate that this mode includes a significant N-H, out-of-plane component.<sup>5</sup> A weak band of  $964\text{ cm}^{-1}$  seems to be due to the  $bR_{570}$  isomer alone. We cannot observe bands below  $750\text{ cm}^{-1}$  because of the limitations of the filter cutoff.

#### *Deuteration Studies of $bR_{560}^{DA}$*

Suspension of purple membrane in  $D_2O$  has no apparent effect upon the  $1,100\text{--}1,400\text{-cm}^{-1}$  fingerprint region (20). The Schiff base frequency in both dark-adapted forms shifts from

<sup>5</sup>Warshel, A. Private communication.

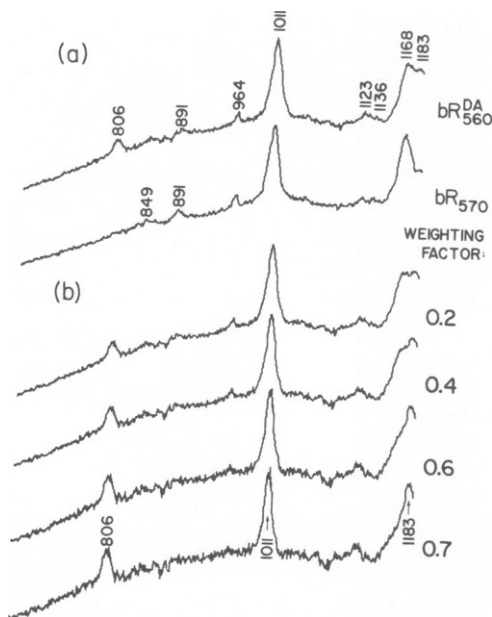


FIGURE 10

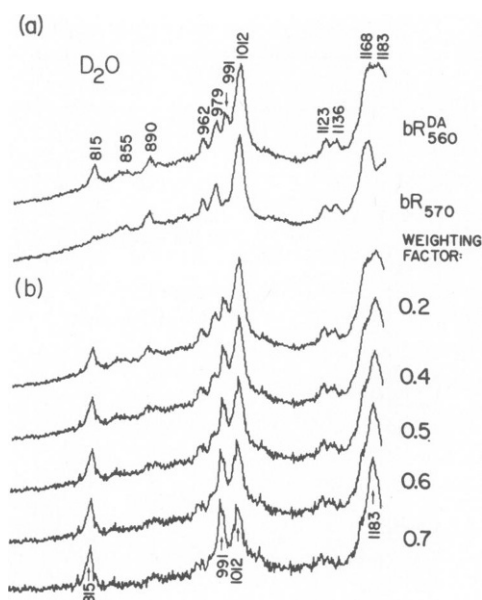


FIGURE 11

FIGURE 10 (a) Comparison of the resonance Raman spectra of dark-adapted  $bR_{560}^{DA}$  and light-adapted  $bR_{570}$  using 1 mW of 5,287 Å excitation and a recirculating flow sample in the range 750–1,150  $\text{cm}^{-1}$ . (b) Computer subtraction of the spectra in a by arbitrary weighting factors leaving the resonance Raman spectrum of  $bR_{550}^{DA}$ .

FIGURE 11 (a) Comparison of the resonance Raman spectra of dark-adapted  $bR_{560}^{DA}$  and light-adapted  $bR_{570}$ , in a  $D_2O$  suspension, in the range 750–1,190  $\text{cm}^{-1}$ , using 1 mW of 5,145 Å excitation and a recirculating flow sample. (b) Computer subtraction of the spectra shown in a by arbitrary weighting factors leaving the resonance Raman spectra of  $bR_{550}^{DA}$  in  $D_2O$ .

1,644 in  $H_2O$  to 1,622 in  $D_2O$  (20). Observation of this shift has been used to assign the protonated Schiff base in bacteriorhodopsin (6) as well as visual pigments.

We have included a  $D_2O$  spectrum for the region 750–1,100  $\text{cm}^{-1}$  (Fig. 11) because of two interesting features. Aside from the 979  $\text{cm}^{-1}$  band of the  $bR_{570}$  form, a new band at 991  $\text{cm}^{-1}$  appears which is unique to  $bR_{550}^{DA}$ . Additionally an 806- $\text{cm}^{-1}$  vibration exhibits an increase in frequency to 815  $\text{cm}^{-1}$  in  $D_2O$ .

## DISCUSSION

### $bL_{550}$

We have based our assignment of the  $bL_{550}$  bands on their kinetic behavior. Our previous work has shown that the  $C=C$  stretch at  $\approx 1,550 \text{ cm}^{-1}$  (8) and a band in the fingerprint region at 1,194  $\text{cm}^{-1}$  (15) have a microsecond rise time and appear before  $bM_{412}$  or  $bO_{640}$ . Though we have not been able to obtain kinetic data on the remaining  $bL_{550}$  bands described in this paper because of their weak intensity, these bands all appear within 10  $\mu\text{s}$  along with the previously assigned bands at 1,550 and 1,194  $\text{cm}^{-1}$ . The  $bM_{412}$  (8) and  $bO_{640}$  intermediates, which are

easily identifiable from our experience, do not present any noticeable contributions to these spectra. There is a contribution to the spectra, however, by  $bK_{590}$ <sup>2</sup> as evidenced by bands at 1,522  $\text{cm}^{-1}$  (Fig. 5), 967 and 986  $\text{cm}^{-1}$  (Fig. 6), 971  $\text{cm}^{-1}$  in  $D_2O$  (Fig. 7) as well as small contributions of intensity to bands in the fingerprint region.

The  $bL_{550}$  intermediate appears to be protonated as evidenced by a band at 1,647  $\text{cm}^{-1}$  which shifts to 1,619  $\text{cm}^{-1}$  upon suspension of the purple membrane in  $D_2O$ . This is confirmed by an additional feature at 988  $\text{cm}^{-1}$  unique to deuterated samples. This laboratory has previously suggested (7) that  $bL_{550}$  may have had an unprotonated Schiff base based on the appearance of a band at 1,620  $\text{cm}^{-1}$  previously assigned to an unprotonated C=N stretching vibration (6). The assignment is probably not based on solid ground. We have now determined that a contribution to the intensity of the 1,620- $\text{cm}^{-1}$  band was in part contributed by the broad water scattering band centered at 1,640  $\text{cm}^{-1}$  but also by the  $bK_{590}$  intermediate<sup>2</sup> which possesses a band at 1,626  $\text{cm}^{-1}$  and is present in significant concentration (10–20%) in the 10  $\mu\text{s}$  spectra using 5,145 Å excitation. The assignment of a protonated Schiff base for  $bL_{550}$  is in agreement with a theoretical study which predicts red-shifted visual pigments to have protonated Schiff bases (25). The deprotonation step in the bacteriorhodopsin cycle is thus the  $bL_{550}$  to  $bM_{412}$  transformation.

The C=C stretching frequency<sup>4</sup> around 1,547  $\text{cm}^{-1}$  (Fig. 5) obtained from the subtracted spectrum follows the inverse linear correlation of  $\nu_{C-C}$  with  $\lambda_{\text{max}}$  of Heyde et al. (23) though it does not fall as closely on the linear plot as some rhodopsins and model compounds (11). In the fingerprint region, the single intense band at 1,197  $\text{cm}^{-1}$  is similar to the large band at 1,180  $\text{cm}^{-1}$  (with a 1,188- $\text{cm}^{-1}$  shoulder) of  $bM_{412}$  (8, 11), even though  $bL_{550}$  is protonated and  $bM_{412}$  is not. The fingerprint regions of  $bL_{550}$  and  $bM_{412}$  appear to have very little in common with the fingerprint region of  $bR_{570}$  except for small bands at 1,255, 1,275, 1,309, and 1,377  $\text{cm}^{-1}$  which are shared with other intermediates<sup>2</sup>. Though rhodopsin and isorhodopsin have been matched well with model 11-*cis*- and 9-*cis*-protonated Schiff bases (14), a similar matching cannot be obtained for  $bL_{550}$ . It may be noted that the single band at 1,197  $\text{cm}^{-1}$  does appear closer to a large band at 1,198  $\text{cm}^{-1}$  of a protonated all-*trans* model (14), than to the other isomers which possess multiple large bands in this region. Bands of  $bL_{550}$  in the region from 1,300 to 1,380  $\text{cm}^{-1}$  do not appear to match closely bands of the all-*trans* model compound in the same region but since most of these bands are shared with all other bacteriorhodopsin forms,<sup>2</sup> these bands may not be indicative of the isomeric configuration.

### $bR_{560}^{DA}$

Dark-adapted bacteriorhodopsin is generally thought to be an equilibrium mixture of two isomers, 13-*cis* and all-*trans* retinal. The spectrum of  $bR_{550}^{DA}$  ( $bR_{570}$  subtracted from  $bR_{560}^{DA}$ ) resembles spectra of neither 13-*cis* nor all-*trans* model compounds published to date, assuming that the subtraction of the spectrum of  $bR_{570}$  from that of  $bR_{560}^{DA}$  is a valid operation. The mode at 806  $\text{cm}^{-1}$  (815  $\text{cm}^{-1}$  in  $D_2O$ ) if it is a torsional mode (24) and the lack of similarity to all-*trans* retinal spectra might suggest that  $bR_{550}^{DA}$  is some sort of *cis* isomer.

Dark-adapted bacteriorhodopsin appears to possess protonated Schiff bases in both equilibrium forms as evidenced by shifts of the 1,644  $\text{cm}^{-1}$  C=N stretching vibration to 1,622  $\text{cm}^{-1}$  upon deuteration. The presence of an exchangeable proton on the chromophore is confirmed by an additional band at 991  $\text{cm}^{-1}$  unique to deuterated samples.

### *Evidence for Retinal Conformational Changes in the Light-Adapted Cycle*

In a previous publication (8), this laboratory noted the similarity of the fingerprint region of  $\text{bR}_{570}$  in the range  $1,160\text{--}1,230\text{ cm}^{-1}$  to the same region of a 13-*cis* retinal protonated model Schiff base (14) even though the  $\text{bR}_{570}$  spectrum possessed an additional feature at  $1,190\text{ cm}^{-1}$  (aside from the high valley between the  $1,173$  and  $1,201\text{-cm}^{-1}$  bands). We have now determined that the "extra"  $1,190\text{-cm}^{-1}$  band is actually a combination of bands belonging to  $\text{bL}_{550}$  and  $\text{bO}_{640}$ .<sup>1</sup> Though the similarity of  $\text{bR}_{570}$  to 13-*cis* retinal is therefore greater than we had previously thought, there are still enough similarities with all-*trans* retinal (14), such that the all-*trans* retinal assignment cannot be ruled out. The difficulty we are presently encountering in making an isomeric assignment might simply be a result of the fact that due to the opsin-retinal interaction, the form or spectrum of the retinal, changes from the corresponding spectrum in solution.

It has been felt that the isomeric configuration of the retinal chromophore during the light-adapted cycle is all-*trans* throughout the light-adapted cycle (26), contrary to the 11-*cis*-to-*trans* isomerization of the visual pigments; although a *trans*-to-*cis* mechanism has recently been suggested (27). Our results show that the fingerprint regions of  $\text{bL}_{550}$  and  $\text{bM}_{412}$  (8, 11) show similarities, having large single bands at  $1,197$  and  $1,180\text{ cm}^{-1}$ , respectively, and are dissimilar to the large triad of bands at  $1,172$ ,  $1,203$ , and  $1,215\text{ cm}^{-1}$  of  $\text{bR}_{570}$ . This suggests that some sort of conformational changes of the chromophore may in fact be occurring during the light-adapted cycle, as well as the dark-adaptation process, which also shows conspicuous changes in this vibrational region. Further modeling and solvent studies as well as theoretical calculations such as those of Warshel and Karplus (24) need to be carried out before conclusive statements can be made about the exact isomeric configurations of the chromophores of  $\text{bL}_{550}$ ,  $\text{bR}_{560}^{\text{DA}}$ , or other intermediates.

The authors are most grateful to Professor Malcolm Nicol and Professor Paul Boyer for the use of their facilities and to Janis Dote and George Phillis for helpful discussions.

The authors acknowledge support from the U.S. Department of Energy, Office of Basic Energy Sciences. James Turner acknowledges a National Science Foundation National Needs Traineeship.

Received for publication 15 August 1978 and in revised form 13 January 1979.

### REFERENCES

1. OESTERHELT, D., and W. STOECKENIUS. 1973. Functions of a new photoreceptor membrane. *Proc. Natl. Acad. Sci. U.S.A.* **70**:2853-2857.
2. HILDEBRAND, E. 1977. What does *Halobacterium* tell us about photoreception? *Biophys. Struct. Mech.* **3**:69-77.
3. STOECKENIUS, W., R. H. LOZIER, and R. A. BOGOMOLNI. 1979. Bacteriorhodopsin and the purple membrane of halobacteria. *Biochim. Biophys. Acta*. **505**:In press.
4. MENDELSON, R. 1973. Resonance Raman spectroscopy of the photoreceptor-like pigment of *Halobacterium halobium*. *Nature (Lond.)* **243**:22-24.
5. MENDELSON, R., A. L. VERMA, H. J. BERNSTEIN, and M. KATES. 1974. Structural studies of bacteriorhodopsin from *Halobacterium cutirubrum* by resonance Raman spectroscopy. *Can. J. Biochem.* **52**:774-781.
6. LEWIS, A., J. SPOONHOWER, R. A. BOGOMOLNI, R. H. LOZIER, and W. STOECKENIUS. 1974. Tunable laser resonance Raman spectroscopy of bacteriorhodopsin. *Proc. Natl. Acad. Sci. U.S.A.* **71**:4462-4466.
7. CAMPION, A., J. TERNER, and M. A. EL-SAYED. 1977. Time-resolved resonance Raman spectroscopy of bacteriorhodopsin. *Nature (Lond.)* **265**:659-661.

8. TERNER, J., A. CAMPION, and M. A. EL-SAYED. 1977. Time-resolved resonance Raman spectroscopy of bacteriorhodopsin on the millisecond timescale. *Proc. Natl. Acad. Sci. U.S.A.* **74**:5212–5216.
9. CAMPION, A., M. A. EL-SAYED, and J. TERNER. 1977. Resonance Raman kinetic spectroscopy of bacteriorhodopsin on the microsecond timescale. *Biophys. J.* **20**:369–375.
10. MARCUS, M. A., and A. LEWIS. 1977. Kinetic resonance Raman spectroscopy: Dynamics of the deprotonation of the Schiff base of bacteriorhodopsin. *Science (Wash. D. C.)* **195**:1328–1330.
11. ATON, B., A. G. DOUKAS, R. H. CALLENDER, B. BECHER, and T. G. EBERGY. 1977. Resonance Raman studies of the purple membrane. *Biochemistry*. **16**:2995–2999.
12. MATHIES, R., A. R. OSEROFF, and L. STRYER. 1976. Rapid-flow resonance Raman spectroscopy of photolabile molecules: rhodopsin and isorhodopsin. *Proc. Natl. Acad. Sci. U.S.A.* **73**:1–5.
13. CALLENDER, R. H., A. DOUKAS, R. CROUCH, and K. NAKANISHI. 1976. Molecular flow resonance Raman effect from retinal and rhodopsin. *Biochemistry*. **15**:1621–1629.
14. MATHIES, R., T. B. FREEDMAN, and L. STRYER. 1977. Resonance Raman studies of the conformation of retinal in rhodopsin and isorhodopsin. *J. Mol. Biol.* **109**:367–372.
15. TERNER, J., and M. A. EL-SAYED. 1978. Time-resolved resonance Raman characterization of the intermediates of bacteriorhodopsin. *Biophys. J.* **24**:262–264.
16. BECHER, B. M., and J. Y. CASSIM. 1975. Improved isolation procedures for the purple membrane of *Halobacterium halobium*. *Prep. Biochem.* **5**:161–178.
17. HURLEY, J. B., B. BECHER and T. G. EBREY. 1978. Evidence that light isomerises the chromophore of purple membrane protein. *Nature (Lond.)* **272**:87–88.
18. GABER, B. P., P. YAGER, and W. L. PETICOLAS. 1978. Interpretation of biomembrane structure by Raman difference spectroscopy. Nature of the endothermic transitions in phosphatidylcholines. *Biophys. J.* **21**:161–176.
19. MARCUS, M. A., and A. LEWIS. 1978. Resonance Raman spectroscopy of the retinylidene chromophore in bacteriorhodopsin (bR<sub>570</sub>), bR<sub>560</sub>, bM<sub>412</sub>, and other intermediates: structural conclusions based on kinetics, models and isotropically labelled membranes. *Biochemistry*. **22**:4722–4735.
20. TERNER, J. 1978. Time-resolved resonance Raman spectroscopy of bacteriorhodopsin. Ph.D. thesis. University of California, Los Angeles, Los Angeles, California.
21. DENCHER, N. A., Ch. N. RAFFERTY, and W. SPERLING. 1976. 13-*cis* and *trans* bacteriorhodopsin: photochemistry and dark equilibrium. *Berichte der Kernforschungsanlage Jülich, Jü-1374*: 1–42 December, 1976.
22. SPERLING, W., P. CARL, Ch. N. RAFFERTY, and N. A. DENCHER. 1977. Photochemistry and dark equilibrium of retinal isomers and bacteriorhodopsin isomers. *Biophys. Struct. Mech.* **3**:79–94.
23. HEYDE, M. E., D. GILL, R. G. KILPONEN, and L. RIMAI. 1971. Raman spectra of Schiff bases of retinal (models of visual photoreceptors). *J. Am. Chem. Soc.* **93**:6776–6780.
24. WARSHEL, A., and M. KARPUS. 1974. Calculation of  $\pi\pi^*$  excited state conformations and vibronic structure of retinal and related molecules. *J. Am. Chem. Soc.* **96**:5677–5689.
25. HONIG, B., A. D. GREENBERG, V. DINUR, and T. G. EBREY. 1976. Visual-pigment spectra: implications of the protonation of the retinal Schiff base. *Biochemistry*. **15**:4593–4599.
26. LEWIS, A. 1978. The molecular mechanism of excitation in visual transduction and bacteriorhodopsin. *Proc. Natl. Acad. Sci. U.S.A.* **75**:548–553.
27. PETTEI, M. J., A. P. YUDD, K. NAKANISHI, R. HENSELMAN, and W. STOECKENINS. 1977. Identification of retinal isomers isolated from bacteriorhodopsin. *Biochemistry*. **16**:1955–1959.